

Article

Thirty-Year Dynamics of LULC at the Dong Thap Muoi Area, Southern Vietnam, Using Google Earth Engine

Nguyen An Binh ¹, Huynh Song Nhut ¹, Nguyen Ngoc An ¹, Tran Anh Phuong ¹, Nguyen Cao Hanh ¹,
Giang Thi Phuong Thao ¹, The Trinh Pham ², Pham Viet Hong ³, Le Thi Thu Ha ⁴, Dieu Tien Bui ^{5,*} 
and Pham Viet Hoa ¹

- ¹ Ho Chi Minh City Institute of Resources Geography, Vietnam Academy of Science and Technology, Ho Chi Minh City 700000, Vietnam; nabinh@hcmig.vast.vn (N.A.B.); hsnhut@hcmig.vast.vn (H.S.N.); nnan@hcmig.vast.vn (N.N.A.); taphuong@hcmig.vast.vn (T.A.P.); nchanh@hcmig.vast.vn (N.C.H.); gtpthao@hcmig.vast.vn (G.T.P.T.); pvhoa@hcmig.vast.vn (P.V.H.)
- ² Dak Lak Department of Science and Technology, Buon Ma Thuot City, Dak Lak 630000, Vietnam; trinhkhcn@yahoo.com
- ³ Institute of Marine Geology and Geophysics, Vietnam Academy of Science and Technology, Hanoi 100000, Vietnam; hc18052001@yahoo.com
- ⁴ Department of Surface Mining, Hanoi University of Mining and Geology, Bac Tu Liem District, Hanoi 100000, Vietnam; lethithuha@hmg.edu.vn
- ⁵ GIS Group, Department of Business and IT, University of South-Eastern Norway, N-3800 Bø i Telemark, Norway
- * Correspondence: dieu.t.bui@usn.no



Citation: Binh, N.A.; Nhut, H.S.; An, N.N.; Phuong, T.A.; Hanh, N.C.; Thao, G.T.P.; Pham, T.T.; Hong, P.V.; Ha, L.T.T.; Bui, D.T.; et al. Thirty-Year Dynamics of LULC at the Dong Thap Muoi Area, Southern Vietnam, Using Google Earth Engine. *ISPRS Int. J. Geo-Inf.* **2021**, *10*, 226. <https://doi.org/10.3390/ijgi10040226>

Academic Editor: Wolfgang Kainz

Received: 31 January 2021

Accepted: 23 March 2021

Published: 6 April 2021

Publisher's Note: MDPI stays neutral with regard to jurisdictional claims in published maps and institutional affiliations.



Copyright: © 2021 by the authors. Licensee MDPI, Basel, Switzerland. This article is an open access article distributed under the terms and conditions of the Creative Commons Attribution (CC BY) license (<https://creativecommons.org/licenses/by/4.0/>).

Abstract: The main purpose of this paper is to assess the land use and land cover (LULC) changes for thirty years, from 1990–2020, in the Dong Thap Muoi, a flooded land area of the Mekong River Delta of Vietnam using Google Earth Engine and random forest algorithm. The specific purposes are: (1) determine the main LULC classes and (2) compute and analyze the magnitude and rate of changes for these LULC classes. For the above purposes, 128 Landsat images, topographic maps, land use status maps, cadastral maps, and ancillary data were collected and utilized to derive the LULC maps using the random forest classification algorithm. The overall accuracy of the LULC maps for 1990, 2000, 2010, and 2020 are 88.9, 83.5, 87.1, and 85.6%, respectively. The result showed that the unused land was dominant in 1990 with 28.9 % of the total area, but it was primarily converted to the paddy, a new dominant LULC class in 2020 (45.1%). The forest was reduced significantly from 14.4% in 1990 to only 5.5% of the total area in 2020. Whereas at the same time, the built-up increased from 0.3% to 6.2% of the total area. This research may help the authorities design exploitation policies for the Dong Thap Muoi's socio-economic development and develop a new, stable, and sustainable ecosystem, promoting the advantages of the region, early forming a diversified agricultural structure.

Keywords: land use and land cover; remote sensing; Dong Thap Muoi; Vietnam

1. Introduction

River deltas are considered to be some of the most favorable areas for crowded residential communities in the world, as they cover only around 5% of the total land area globally but are home to more than 500 million people [1]. However, these deltas have been recognized as the main places for significant land use and land cover (LULC) changes due to population growth, urbanization, anthropogenic activities, and socioeconomic development [2]. Over the last decade, these changes have affected various global issues, both positive and negative, including terrestrial ecosystems [3], land surface temperatures [4], regional climates [5], soil quality [6], hydrological regimes [7], flooding [8,9], other natural hazards [10,11], and especially food security [12,13]; therefore, studying LULC changes and assessing driving factors to balance the correlation between the human needs and negative consequences are vital factors for sustainable development [14].

For the world's third-largest delta, the Mekong River Delta, the LULC has changed tremendously over the last four decades due to socioeconomic developments [15]. Although this delta accounts for only 12% of the total area in Vietnam, it contributes to nearly 90% of the total rice exports in Vietnam [16]. It should be noted that in 2019, Vietnam was the third-largest rice exporter in the world [17]. Therefore, studies on LULC changes have a vital role in land use planning and natural resource management [18]. However, only a few studies have been carried out to assess LULC dynamics in this area. Sakamoto et al. [19] used Moderate Resolution Imaging Spectroradiometer (MODIS) images to assess the expansion of shrimp ponds and triple rice areas from 2000 to 2006 in the southeastern part of the delta. Several works were conducted for: (1) the southern part [15,20,21], i.e., in Ca Mau province, where inland agriculture and mangrove plants are dominant; (2) the western part, containing grassland [22]; (3) the eastern part [23]; (4) and across the whole region, such as in [2,14,24,25]. In general, the above studies focused on change assessments over short periods. In addition, LULC changes in the last five years have not been addressed for the Mekong River Delta. More importantly, to the best of our knowledge, no studies have detected and assessed LULC changes for the Dong Thap Muoi area, the delta's lowest land area.

The Dong Thap Muoi area is located in the upper and middle regions of the Mekong Delta. It is also known as a flood plain and is directly influenced by annual floods in the rainy season and the Mekong's hydrological regime [26]. This is an important area because it contributes to about 20% of Vietnam's total rice export volume annually [27]. Exploitation started in this area in the 1980s, before which time it composed of unexploited land dominated by acid sulfate soil, with long-lasting annual floods [28]. After 30 years of exploitation, the Dong Thap Muoi area now greatly contributes to the food supply, ensuring Vietnam's national food security and rice exports [28]. Therefore, assessment of the LULC changes in this area is vital, which will help the authorities design exploitation and socioeconomic development policies in the future.

In LULC change analysis, a lack of accurate GIS data is a big issue, especially in developing countries, as accurate, long-time-series data availability is a must. To date, remote sensing images have been the most widely and efficiently used data [29]. The recent developments in artificial intelligence and cloud computing, i.e., Microsoft Azure Cloud [30], Google Earth Engine (GEE) [31], Geospatial Amazon Web Services [32,33], and Open Data Cube [34], have made it easier to derive LULC classes from remotely sensed data. Herein, using GEE, historical imagery data are accessed and processed online using semi-automatic and automatic workflows [35]. More importantly, powerful algorithms, i.e., random forest methods and other TensorFlow machine learning approaches, are integrated for image classification.

This project's main objective is to assess the LULC changes in the Dong Thap Muoi area during the last three decades, from 1990–2020, using Google Earth Engine and random forest algorithms. Specific objectives are focused on: (1) the study and determination of the main LULC classes for 1990, 2000, 2010, and 2020; (2) assessing the magnitude and rate of changes for these LULC classes; (3) mapping the spatial and temporal changes for different periods (1990–2000, 1990–2010, 1990–2020, 2000–2010, 2000–2020, and 2010–2020). Finally, the results are discussed and conclusions are drawn.

2. Study Area and Data

2.1. Study Area

The Dong Thap Muoi area is located in the lowland part of the Mekong River Delta in the south of Vietnam. Dong Thap Muoi covers an area of 7306.6 km², between longitudes of 105°10' E and 106°34' E and latitudes of 10°19' N and 11°03' N. It is located around 20 km to the west of Ho Chi Minh city, the biggest city in Vietnam. Administratively, Dong Thap Muoi is spread across 19 districts and towns in three provinces, namely Dong Thap (Cao Lanh town and six districts), Long An (eight districts), and Tien Giang (four districts) (Figure 1).

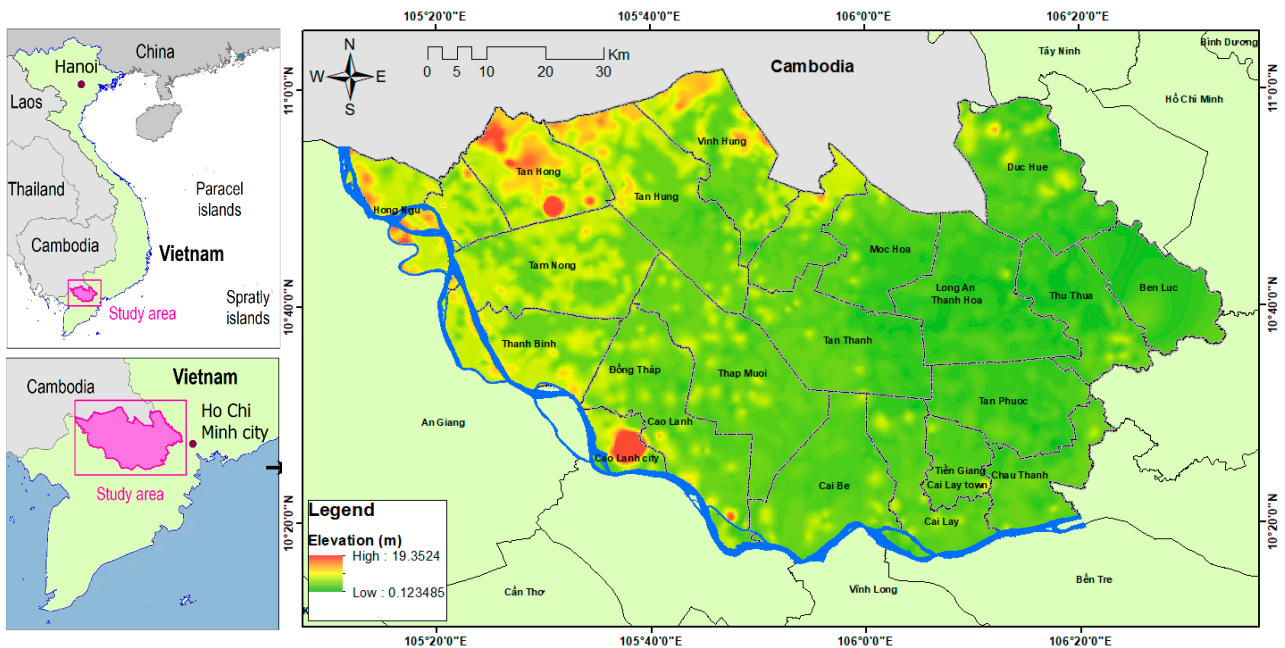


Figure 1. Location of the Dong Thap Muoi area.

The terrain of Dong Thap Muoi is generally flat, with around 73% of the total area between altitudes of 0.5 and 1.25m, whereas areas with an altitude over 2 m occupy only about 7% and the lowest areas with altitudes of 0–0.5m account for only 0.57% of the total area [36]. Regarding the soil, acid sulfate soils cover approximately 39% of the total area, followed by alluvial soil (34.71%), gray soils (16.10%), sandy soils (0.51%), and peat soils (0.02%) [36]. Due to its topographical characteristics, Dong Thap Muoi is a closed flood plain and is strongly influenced by the semi-diurnal tide regime of the East Vietnam Sea. Thus, regular floods, droughts, and acid sulfate problems are major environmental issues, affecting agricultural production and people's lives in the area. Although Dong Thap Muoi covers only 17.7% of the Mekong River Delta area, it occupied 36.7% of the delta's total flooded area [36]. In a normal year, drought and saline intrusion occur between January and April, followed by acid sulfate problems, which occur from May to July, while August to November is the flood season [37,38].

The Dong Thap Muoi climate is characterized by tropical monsoons, being hot, sunny, and high in humidity. This area has only two distinct seasons: rainy and dry seasons. The total yearly precipitation fluctuates in the range of 1300–1700 mm, with the rainy season from May to October accounting for up to 90% of the yearly precipitation [39]. In general, the whole region has a high annual average temperature and is stable in space and time. According to the climate statistics from 1978–2019 at the Cao Lanh station in the study area, the highest and lowest mean annual temperatures were 26.7 and 27.9 °C, respectively. April and January are the months with the highest and lowest average temperatures, respectively.

According to the statistical analysis at Cao Lanh station during 1978–2019, the lowest measured temperature was 15.8 °C in 1986, whereas the highest temperature observed was 37.4 °C in 1983. Regarding the wind regime, the southwest wind from the Gulf of Thailand, usually from May to November, is dominant. This wind is steamy, and therefore causes rain. Meanwhile, the prevailing northeast monsoon season from November to January is usually dry [36]. The average wind speed is 2–2.5 m/s.

2.2. Remote Sensing Images, Ancillary Maps, and Fieldwork Data

In order to cover the Dong Thap Muoi area, a total of 128 scenes with 30 m resolution in the 04 paths and rows (125/052, 125/053, 126/052, and 126/053) were derived from the freely available data catalog in Google Earth Engine (GEE) (<https://developers.google.com/earth-engine/>).

[com/earth-engine/datasets/catalog](https://earth-engine/catalog) (Accessed date: 20 September 2020)). Among the 128 scenes, 98 Landsat-5 scenes were taken from 1990, 2000, 2001, and 2010, whereas 3 Landsat 8 OLI (Operational Land Imager) scenes were taken from 2020. Herein, Landsat 7 images were not considered due to parallel stripe problems. We selected the images from the dry seasons (January to April) of the aforementioned years to minimize the influence of the cloud coverage and the effects of moisture and evaporation on the ground. Nevertheless, the area was still influenced by cloud cover for the years 2000 and 2010, so in order to fix this we used 23 and 14 Landsat-5 scenes for the years 2001 and 2011 for the pixel value recovery processing to derive the full images from 2000 and 2010 for the Dong Thap Muoi area. A detailed description of the Landsat images used in this project is shown in Table 1.

Table 1. Landsat surface reflectance images used to derive the land use and land cover (LULC) changes for the Dong Thap Muoi area. ETM: Enhanced Thematic Mapper. OLI: Operational Land Imager.

Sensor and Image	Path/Row	Acquired Date (Date/Month)	Year
Landsat-5 ETM (19 scenes)	125/052	03/01; 19/01; 04/02; 20/02; 08/03; and 09/04	1990
	125/053	03/01; 19/01; 04/02; and 09/02	1990
	126/052	10/01; 26/01; 27/02; and 16/04	1990
	126/053	10/01; 26/01; 27/02; 15/03; and 16/04	1990
Landsat-5 ETM (28 scenes)	125/052	15/01; 31/01; 16/02; 03/03; 19/03; 04/04; and 20/04	2000
	125/053	15/01; 31/01; 16/02; 03/03; 19/03; 04/04; and 20/04	2000
	126/052	06/01; 22/01; 07/02; 23/02; 10/3; 26/03; 11/04; and 27/04	2000
	126/053	22/01; 23/02; 10/3; 26/03; 11/04; and 27/04	2000
Landsat-5 ETM (23 scenes)	125/052	02/02; 18/02; 06/03; 22/03; 07/04; and 23/04	2001
	125/053	02/02; 18/02; 06/03; 22/03; 07/04; and 23/04	2001
	126/052	08/01; 24/01; 09/02; 29/03; 14/04	2001
	126/053	08/01; 24/01; 09/02; 13/03; 29/03; and 14/04	2001
Landsat-5 ETM (14 scenes)	125/052	26/01; 11/02; 27/02; and 31/03	2010
	125/053	26/01; 11/02; and 27/02	2010
	126/052	17/01; 02/02; and 22/03	2010
	126/053	17/02; 02/02; 18/02; and 12/03	2010
Landsat-5 ETM (14 scenes)	125/052	13/01; 29/01; 02/03; and 18/03	2011
	125/053	29/01 and 02/03	2011
	126/052	20/01; 05/02; 21/02; and 09/03	2011
	126/053	20/01; 05/02; 21/02; and 09/03	2011
Landsat-8 OLI (30 scenes)	125/052	06/01; 22/01; 07/02; 23/02; 10/03; 26/03; 11/04; and 27/04	2020
	125/053	06/01; 22/01; 07/02; 23/02; 10/03; 26/03; 11/04; and 27/04	2020
	126/052	12/01; 29/01; 14/02; 01/03; 17/03; 02/04; 18/04	2020
	126/053	12/01; 29/01; 14/02; 01/03; 17/03; 02/04; 18/04	2020

To support this LULC analysis, certain GIS data layers for the Dong Thap Muoi area, such as the digital elevation model (DEM), district and province boundaries, road networks,

river networks, residential areas, and land uses, were also used. In this project, the ALOS DEM with 30 m resolution was downloaded from the Japan Aerospace Exploration Agency (JAXA) website (<https://www.eorc.jaxa.jp>, assessed on 2 April 2020). The boundaries, road networks, and river networks were derived from the national spatial data infrastructure of the Vietnam Ministry of Natural Resources and Environment (V-MONRE) [40]. For 1990, 2000, 2010, and 2020, 1:2000 cadastre maps provided by the local authorities, land use status maps, and topographic maps compiled by V-MONRE were used for comparisons with fieldwork results. The other ancillary data used in this project are shown in Table 2.

Table 2. The ancillary data used. ALOS DEM: The Advanced Land Observing Satellite digital elevation model.

No.	Ancillary Data	Scale/Resolution	Source
1	Topographic maps	1:50,000	V-MONRE [40]
2	Land use status maps	1:50,000	V-MONRE [40]
	Cadastre maps 1:2000	1:2000	Local authorities
3	ALOS DEM	30 × 30 m	JAXA, https://www.eorc.jaxa.jp (assessed on 2 April 2020)
4	Google Earth Imagery	-	Google LLC, https://www.google.com/earth (assessed on 2 April 2020)
5	Statistical data	-	General Statistics Office of Vietnam, https://www.gso.gov.vn/ (assessed on 2 April 2020)
6	Fieldwork data for June 2020	-	422 samples
7	Humidity and temperature data	1990–2019	Cao Lanh and Moc Hoa stations

The fieldwork was conducted in May and June 2020 using a Trimble handheld GNSS receiver, while an iGeoTrans app [41] installed on an iPad was used to collect samples using the random sampling method [42]. A sampling unit of 30 × 30 m was adopted to the spatial resolution of the Landsat images. Herein, the study area's road network overlaid on Google Earth was used to support the designed field trips. A total of 6 individuals separated into 3 groups conducted these field trips, visiting and checking 422 specific sites covering all of the LULC classes in the Dong Thap Muoi area. These specific sites are spread over 700 km of the roads in the study area. The distribution of the fieldwork sites is shown in Figure 2, while some image samples from the Landsat images are shown in Figure 3. Photos of some LULC classes taken during the fieldwork in the study area are shown in Figure 4. During the field trips, interviews were also carried out with local leaders of communes, village heads, forest ranger staff, and elders.

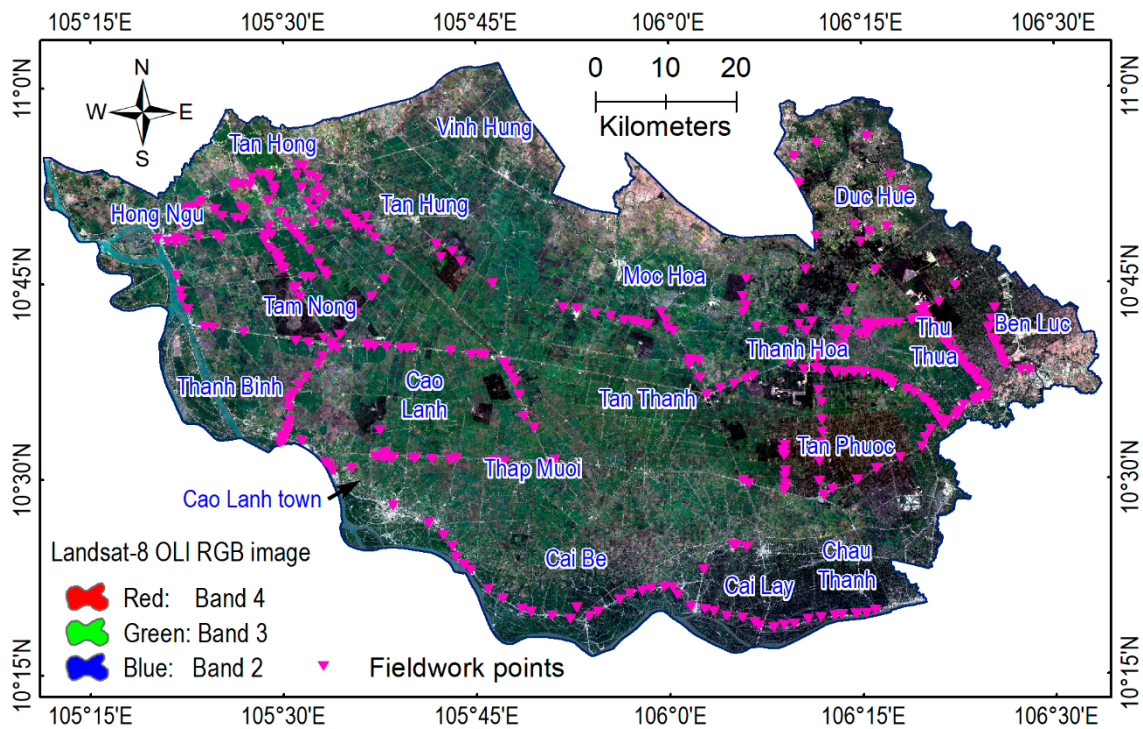


Figure 2. Locations of the fieldwork sites from April 2020 in the Dong Thap Muoi area. OLI: Operational Land Imager. RGB: Read, Green, and Blue.

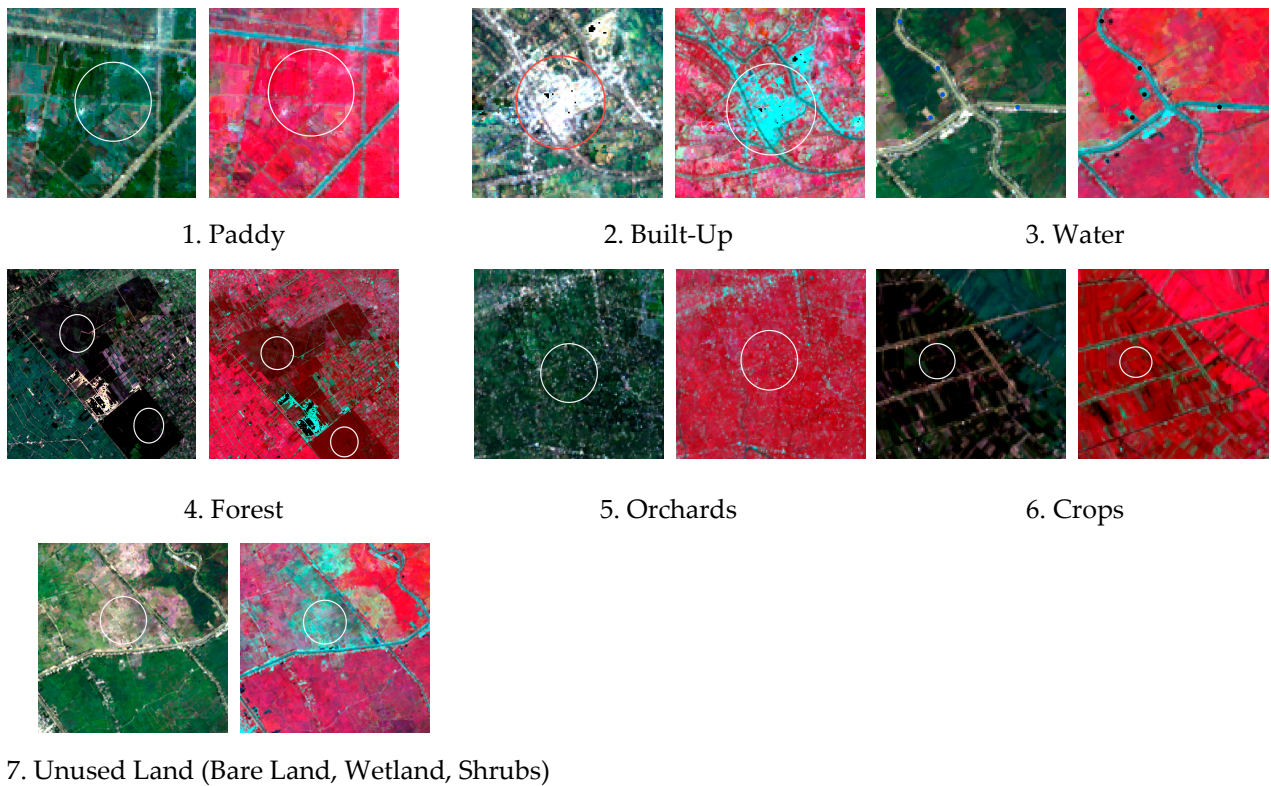


Figure 3. Samples were taken from the Landsat images of the Dong Thap Muoi area. For each class, the left image is the natural RGB band combination, while the right image is the false composite with the NIR band for red color, the red band for green color, and the green band for blue color.



Figure 4. Photos from the field trip in the Dong Thap Muoi area. These photos were taken by Nguyen An Binh and Pham Viet Hoa in May and June 2020.

3. Research Methodology

3.1. Image Pre-Processing

As mentioned above, the Landsat images for the aforementioned years were derived from the freely available GEE. These images were processed and corrected to surface reflectance values, which included corrections for the solar zenith and irradiance, sun, and atmosphere [43,44]. Because the Dong Thap Muoi is a flat area with very low terrain variation, topographic correction with a DEM for this area was not necessary [15,45]. In

this project, the pre-processing was carried out in 8 steps; (1) creation of image data file; (2) cloud filtering; (3) creation of average image of study area; (4) selection of image bands and computation of NDVI (Normalized Difference Vegetation Index) and NDWI (Normalized Difference Water Index) for classification; (5) preparation of LULC classes, followed by training and validation of samples; (6) classification LULC using the random forest approach; (7) accuracy assessment; (8) post-processing and analysis.

For the classification, five bands (blue, red, green, NIR (Near Infrared band), and SWIR (Short-Wave infrared)) of Landsat-5 were used, whereas for Landsat 8 OLI, NDVI and NDWI were additionally computed and utilized. For the post-processing, the final classified images were geometrically corrected to the VN-2000 (Viet Nam 2000) system (zone 48, UTM map projection, ellipsoid WGS84) [46] using the nearest-neighbor sampling algorithm [47]. The purpose of this geometrical correction was to ensure the best alignment between these images and the other spatial data. It is noted that VN-2000 is the national coordinate reference system of Vietnam, which has been officially used since the year 2000 [46]. Herein, topographic maps at 1:50,000 scale (refer to Table 2) were used for this image-to-map registration, and root mean squared error (RMSE) accuracy values below 0.5 pixels [15] were accepted

3.2. Determination of the LULC Classes, Training and Validation of Samples

In this research, the LULC classes for the Dong Thap Muoi area were determined based on the regulations for mapping and updating land use status maps in Vietnam [48], on our fieldwork, and on the land use statistics available for this area. In addition, the instructions for land cover classification of the Food and Agriculture Organization (FAO) [49] and The United States Geological Survey (USGS) land cover database [50] were considered. As a result, a total of 8 broad LULC classes (paddy, built-up, water, forest, orchards, crops, unused land (bare land, wetland, shrubs), and others) were determined (Figures 3 and 4 and Table 3). We used only 8 LULC classes here to raise the probability of the changes are true, whereas ambiguities of categorical differentiation could be reduced.

Table 3. Detailed descriptions of the LULC classes for the Dong Thap Muoi area.

No	LULC Classes	Description
1	Paddy	Rice crops
2	Built-up	Urban built-up areas, roads
3	Water	Rivers, streams, lakes, and canal systems
4	Forest	Productive and natural forests
5	Orchards	Gardens with orange, lemon, pomelo, and mixed fruits
6	Crops	Corn and vegetables
7	Unused Land	Uncultivated land, undeveloped land, new land
8	Others	Clouds, scrub

For supervised classification, it is necessary to prepare training and validation samples. In this project, we selected these samples for the years 1990, 2000, 2010, and 2020 from 1:50,000 topographic maps, 1:50,000 land use status maps, and 1:2000 cadastre maps of the study area. Herein, we used the procedure proposed by Fortier et al. [51] with the random stratification method [52] for the selection. First, Landsat images for 1990, 2000, 2010, and 2020 were placed over these maps in ArcGIS Pro. Then, invariant areas in the eight LULC classes were determined and polygons were drawn in the centers of these areas. Finally, the labels for LULC classes were checked using the three map types listed above. As a result, a total of 1397 samples in the eight LULC classes for the years 1990, 2000, and 2010 were generated using the three ancillary maps for training models with the random forest algorithm. For 2020, only 975 samples were generated using the above ancillary maps, whereas 422 samples were derived through our field trips in June 2020.

3.3. Landsat Image Classification and Accuracy Assessment

Due to the 30 m resolution of the Landsat images used, a pixel-based supervised classification approach was adopted to derive LULC classes for the Dong Thap Muoi area. Since LULC class quality depends on the method or algorithm used and decision tree ensembles have proven to be efficient due to their high accuracy and resistance to noise [53–55], in this research the random forest approach was selected.

The random forest method is a powerful classification scheme proposed by Breiman [56], which has been successfully used in various LULC classification projects [53,57–61]. As pointed out by Sheykhmousa et al. [57], the main advantage of RF is that it can provide very high classification results, and in addition this algorithm is robust to outliers and works well in noisy environments [53]. The working mechanism for RF can be summed up as follows: first, using the LULC training samples, this algorithm separates the training samples into subsets with the use of the bagging technique [62]. Then, each subset is utilized to construct a subtree classifier. Finally, all subtree classifiers are aggregated to create the final forest model. Overall, the random forest model's classification power is strongly influenced by the number of subtrees used, as a result of its diverse characteristics; therefore, this parameter should be carefully considered. As suggested in previous works [63–65], a total of 500 subtrees were used in this project.

For the accuracy assessment of the LULC maps in this project, both qualitative and quantitative methods were adopted. For the qualitative assessment, the LULC maps for the years 1990, 2000, 2010, and 2020 and their corresponding Landsat images were overlaid over topographic maps, land use status maps, and cadastre maps, then visual checks and assessments were carried out. For the quantitative verification, the LULC map quality was checked using various well-known and widely accepted statistical measures (i.e., kappa index; user, producer, and overall accuracy values), as mentioned in [42,66]. A detailed explanation of these statistical measures can be found in [42,47].

3.4. LULC Change Assessment

The final LULC classification maps for the four years (1990, 2000, 2010, and 2020) outlined in Section 3.3 were then post-processed in ArcGIS Pro. Herein, LULC changes for six different periods (1990–2000, 1990–2010, 1990–2020, 2000–2010, 2000–2020, and 2010–2020) were computed. Finally, the change matrices and change pattern maps for these periods were derived.

4. Results and Analysis

4.1. LULC Classification and Accuracy

A total of four random forest models for 1990, 2000, 2010, and 2020 for the Dong Thap Muoi area were successfully constructed and validated. The results are shown in Tables 4 and 5. It can be seen that the overall accuracy (OA) values for the years 1990, 2000, 2010, and 2020 were 88.93, 83.47, 87.18, and 82.37%, respectively; whereas the kappa index values were 0.889 for 1990, 0.835 for 2000, 0.872 for 2010, and 0.824 for 2020. These results indicate that these random forest models fit well with the datasets at hand. The ability of these models to classify new pixels is shown in Table 5. The OA values for the years 1990, 2000, 2010, and 2020 were 88.93, 83.47, 87.18, and 82.37%, respectively; whereas the kappa index values ranged from 0.751 (2010) to 0.803 (1990), indicating satisfactory results. The remaining detailed results are depicted in Tables 4 and 5.

Table 4. Accuracy assessment for the LULC maps of the Dong Thap Muoi area, assessed using the training samples. OA: overall accuracy.

Year	Accuracy	LULC Classes							OA	Kappa Index
		Paddy	Built-Up	Water	Forest	Orchards	Crops	Unused Land		
1990	Producer	84.5	81.8	97.2	92.5	83.9	82.1	91.1	88.9	0.889
	User	78.9	85.7	96.6	90.2	82.1	96.0	88.1		
2000	Producer	83.0	70.6	91.5	90.2	85.8	77.1	78.1	83.5	0.835
	User	86.5	76.6	91.5	86.5	79.2	77.1	80.9		
2010	Producer	90.1	71.4	92.2	86.5	84.3	91.5	86.2	87.1	0.871
	User	91.9	75.0	89.2	90.1	80.4	96.2	83.5		
2020	Producer	87.3	81.1	90.0	83.3	94.7	85.0	65.2	85.6	0.856
	User	88.0	82.6	90.8	87.4	82.4	89.7	66.7		

Table 5. The extent of the LULC classes in the Dong Thap Muoi area for the period 1990–2020.

LULC Class	Area (km ²)			
	1990	2000	2010	2020
1. Paddy	935.0	1874.5	2941.4	3292.2
2. Built-up	18.8	35.3	162.5	450.7
3. Water	403.6	292.6	416.1	491.3
4. Forest	1049.5	733.9	696.5	402.7
5. Orchards	1322.0	1433.4	1186.0	1257.7
6. Crops	1462.4	2085.8	1305.3	1170.0
7. Unused land	2111.9	849.8	543.7	236.0
8. Others	3.4	1.2	55.0	5.9

4.2. LULC Estimation

The final trained random forest models were used to derive the spatial patterns for eight LULC classes (paddy, built-up, water, forest, orchards, crops, unused land, and others) for the years 1990, 2000, 2010, and 2020. The results are shown in Figure 5 and Table 5.

It can be seen that the most dramatic change in the area is for the paddy classification, as it occupied only 935.0 km² in 1990 but steadily increased to 1874.5 km² in 2000, 2941.4 km² in 2010, and 3292.2 km² in 2020. Inversely, the unused land areas, located mainly in the north, crossing the border between Vietnam and Cambodia, covered 2111.9 km² in 1990 but were strongly reduced by nearly nine times by 2020 (236.0 km²).

Showing a similar trend but at a slightly reduced level, the forest areas, which were mainly distributed in the northeast part in 1990 (1049.5 km²), were reduced to 402.7 km² by the year 2020 and were located in fragmented clusters. For the crops class, the changes over the past 30 years were different compared to the other LULC classes. Although the crops area increased from 1462.4 km² in 1990 to 2085.8 km² in 2000, it was reduced significantly to 1305.3 km² in 2010 and to only 1170.0 km² in 2020. Regarding the built-up classification, the total area in 1990 was just 18.8 km², with a fragmented pattern, but however it exponentially increased to 35.3 km² in 2000, 162.5 km² in 2010, and 450.7 km² in 2020.

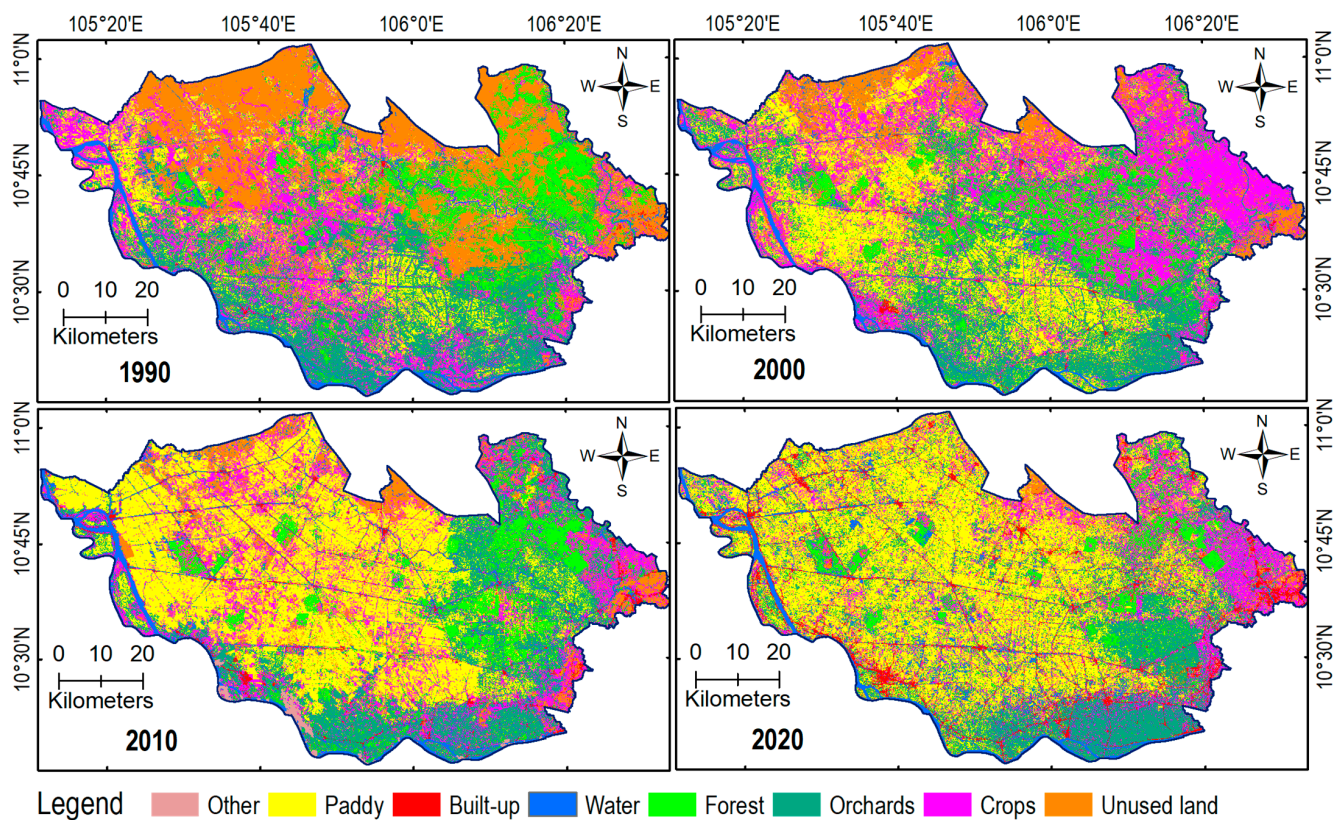


Figure 5. LULC classes in the Dong Thap Muoi area for the different years.

4.3. LULC Evolution Analysis

The evolution of the LULC classes in the Dong Thap Muoi area is shown in Table 6 and Figures 6–8. Among the eight classes, the paddy class showed the largest change, followed by the unused land class. During the period 1990–2020, the paddy area increased by 2357.2 km², whereas the unused land area decreased by 1875.9 km². These changes accounted for 32.3% (paddy) and 25.7% (unused land) of the total studied area. The highest annual rate of change for the paddy class was around 106.7 km²/year for the period 2000–2010, while for the unused land class it was 126.2 km²/year for the period 1990–2000 (Table 6).

Table 6. The magnitudes and annual rate changes for the LULC classes in the Dong Thap Muoi area for the period 1990–2020.

LULC Class	Change Magnitude (km ²)						Change Rate per Year (km ² /Year)					
	1990–2000	1990–2010	1990–2020	2000–2010	2000–2020	2010–2020	1990–2000	1990–2010	1990–2020	2000–2010	2000–2020	2010–2020
1. Paddy	939.6	2006.4	2357.2	1066.8	1417.7	350.8	94.0	100.3	78.6	106.7	70.9	35.1
2. Built-up	16.6	143.8	432.0	127.2	415.4	288.2	1.7	7.2	14.4	12.7	20.8	28.8
3. Water	−111.0	12.5	87.7	123.5	198.7	75.2	−11.1	0.6	2.9	12.3	9.9	7.5
4. Forest	−315.7	−353.0	−646.8	−37.4	−331.1	−293.8	−31.6	−17.7	−21.6	−3.7	−16.6	−29.4
5. Orchards	111.5	−136.0	−64.3	−247.4	−175.8	71.7	11.1	−6.8	−2.1	−24.7	−8.8	7.2
6. Crops	623.4	−157.1	−292.4	−780.6	−915.9	−135.3	62.3	−7.9	−9.7	−78.1	−45.8	−13.5
7. Unused land	−1262.1	−1568.2	−1875.9	−306.1	−613.7	−832.2	−126.2	−78.4	−62.5	−30.6	−30.7	−83.2
8. Others	−2.2	51.6	2.5	53.9	4.7	−49.2	−0.2	2.6	0.1	5.4	0.2	−4.9

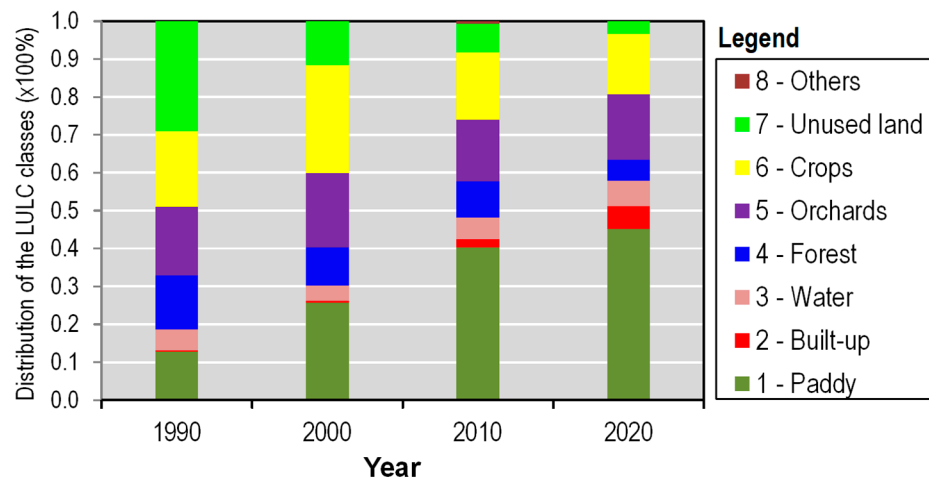


Figure 6. Distribution of LULC classes of the Dong Thap Muoi area in 1990, 2000, 2010, and 2020.

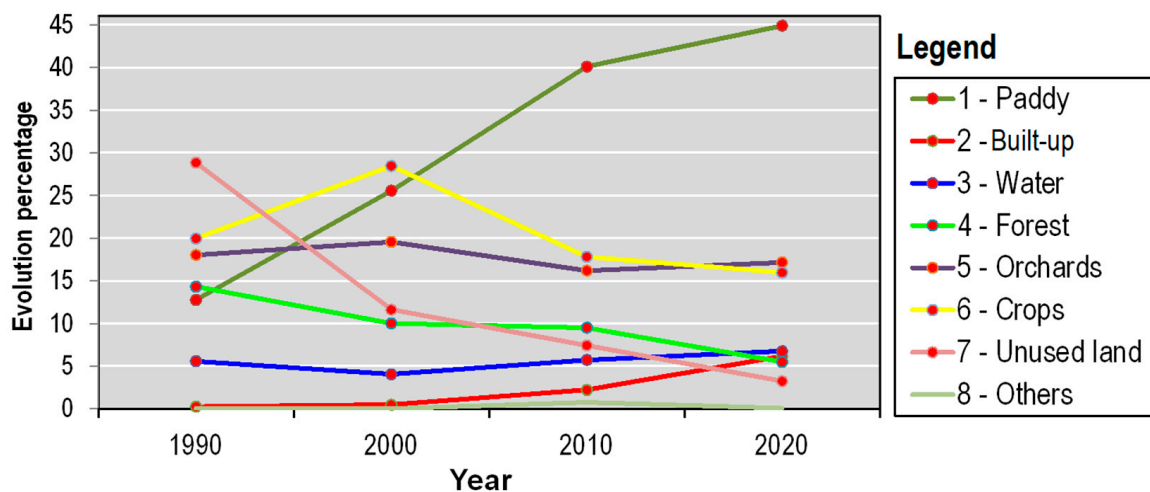


Figure 7. The evolution of the LULC classes in the Dong Thap Muoi for the period 1990–2020.

These magnitude changes were followed by the forest (-646.8 km^2), built-up (432.0 km^2), crops (-292.4 km^2), water (87.7 km^2), and orchard (-64.3 km^2) classes between 1990 and 2020. These changes corresponded to 8.9, 5.9, 4.0, 1.2, and 0.9% of the total studied area. The annual rate of change for the forest was highest ($-31.6 \text{ km}^2/\text{year}$) in the period 1990–2000, which then reduced from 2000 to 2010 ($-3.7 \text{ km}^2/\text{year}$), but increased to $-29.4 \text{ km}^2/\text{year}$ for the 2010–2020 period. Regarding the built-up class, the annual rate of change was high ($20.8 \text{ km}^2/\text{year}$) for the 2000–2020 period, especially from 2010 to 2020, where the rate reached $28.8 \text{ km}^2/\text{year}$. The magnitude and annual rate changes for the other LULC classes are shown in Table 6 and Figures 7 and 8.

Detailed conversions of the LULC changes in the Dong Thap Muoi area are shown in Table 7, which presents the change matrix for the 1990–2020 period over six different time spans. Herein, the diagonal line denotes the number of the LULC classes showing no change, whereas the values above the diagonal line explain the expansion areas. The values below the diagonal line refer to the reduction areas.

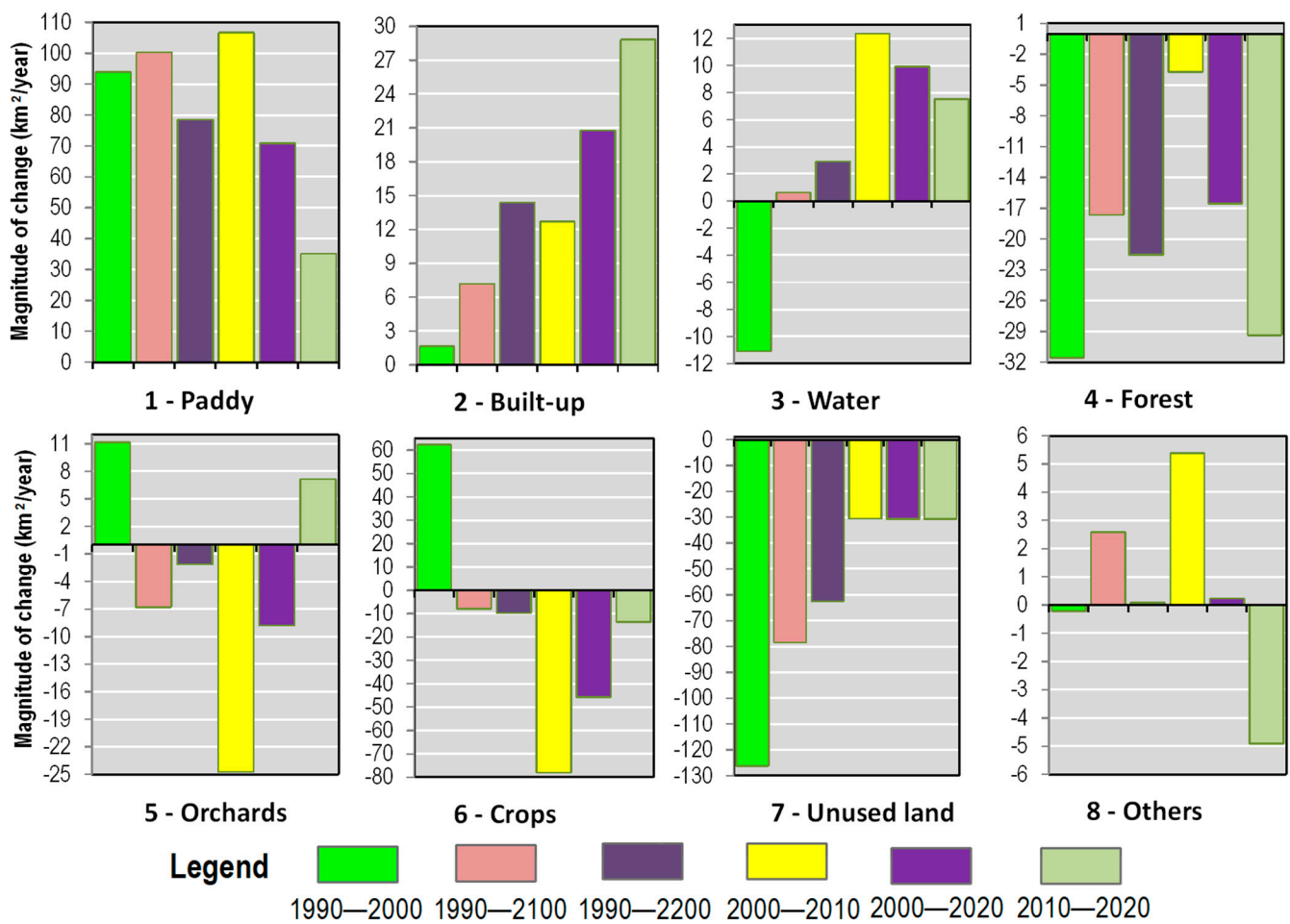


Figure 8. The magnitudes of change for the LULC classes in the Dong Thap Muoi, shown in ha/year, across different time spans.

Table 7. LULC map changes for the Dong Thap Muoi area for the period 1990–2020 with detailed subperiods. Unit: km².

The 1990–2000 Period	PD	BU	WT	FR	OC	CR	UL	OT	Total	Expansion	
2000	Paddy (PD)	454.4	0.9	66.6	150.8	357.1	451.8	392.4	0.5	1874.5	1420.1
	Built-up (BU)	2.3	4.9	1.5	1.2	8.1	8.5	8.7	0.1	35.3	30.4
	Water (WT)	5.9	1.4	177.3	14.2	10.7	21.4	61.2	0.5	292.6	115.3
	Forest (FR)	38.2	0.2	27.1	238.9	128.9	104.8	195.7	0.0	733.9	494.9
	Orchards (OC)	169.3	1.0	43.9	175.0	509.0	362.6	172.5	0.0	1433.4	924.5
	Crops (CR)	209.3	4.6	62.4	390.0	266.8	403.2	749.0	0.5	2085.8	1682.7
	Unused (UL)	55.4	5.7	24.7	79.3	41.3	109.8	531.9	1.6	849.8	317.9
	Others (OT)	0.0	0.0	0.1	0.1	0.1	0.2	0.5	0.1	1.2	1.1
	Total	935.0	18.8	403.6	1049.5	1322.0	1462.4	2111.9	3.4	7306.6	4986.8
	Reduction	480.5	13.8	226.3	810.6	813.0	1059.2	1580.0	3.3	4986.8	0.0

Table 7. Cont.

The 1990–2010 Period		PD	BU	WT	FR	OC	CR	UL	OT	Total	Expansion
2010	Paddy (PD)	588.7	2.1	109.8	364.9	430.2	676.7	768.2	0.8	2941.4	2352.7
	Built-up (BU)	12.7	6.5	5.0	9.7	28.1	43.5	56.4	0.6	162.5	156.0
	Water (WT)	18.3	1.8	166.8	26.9	34.7	63.1	103.7	0.7	416.1	249.4
	Forest (FR)	22.3	0.4	21.9	243.4	133.0	73.7	201.7	0.1	696.5	453.1
	Orchards (OC)	104.5	0.5	31.3	219.7	391.7	207.3	230.9	0.0	1186.0	794.3
	Crops (CR)	138.9	2.7	39.1	146.4	237.1	306.6	433.9	0.5	1305.3	998.7
	Unused (UL)	46.4	4.7	10.1	37.2	45.5	85.3	314.0	0.5	543.7	229.7
	Others (OT)	3.0	0.1	19.7	1.3	21.7	6.1	3.0	0.1	55.0	54.9
	Total	935.0	18.8	403.6	1049.5	1322.0	1462.4	2111.9	3.4	7306.6	5288.7
	Reduction	346.3	12.2	236.8	806.1	930.3	1155.8	1797.9	3.3	5288.7	
The 1990–2020 Period		PD	BU	WT	FR	OC	CR	UL	OT	Total	Expansion
2020	Paddy (PD)	575.3	2.1	121.3	429.2	487.5	701.3	974.4	1.1	3292.2	2717.0
	Built-up (BU)	41.7	9.3	17.7	27.3	105.2	117.0	131.5	0.9	450.7	441.4
	Water (WT)	51.1	0.9	171.4	35.9	52.5	86.7	92.4	0.5	491.3	320.0
	Forest (FR)	17.7	0.2	18.0	142.9	51.8	49.1	123.0	0.1	402.7	259.8
	Orchards (OC)	117.7	1.0	32.1	195.9	419.2	246.3	245.3	0.2	1257.7	838.4
	Crops (CR)	113.6	3.1	27.7	188.7	185.9	233.5	416.9	0.5	1170.0	936.5
	Unused (UL)	17.6	2.0	14.9	28.2	19.3	27.6	126.3	0.1	236.0	109.8
	Others (OT)	0.2	0.2	0.5	1.4	0.4	0.9	2.2	0.0	5.9	5.9
	Total	935.0	18.8	403.6	1049.5	1322.0	1462.4	2111.9	3.4	7306.6	5628.8
	Reduction	359.7	9.5	232.2	906.7	902.7	1228.9	1985.7	3.4	5628.8	
The 2000–2010 Period		PD	BU	WT	FR	OC	CR	UL	OT	Total	Expansion
2010	Paddy (PD)	1163.4	4.8	33.8	278.0	533.1	685.8	242.3	0.1	2941.4	1778.0
	Built-up (BU)	17.1	15.0	7.8	6.5	22.2	61.0	32.7	0.1	162.5	147.5
	Water (WT)	32.6	5.2	169.0	19.9	29.0	104.1	56.2	0.1	416.1	247.1
	Forest (FR)	41.1	1.1	11.4	205.3	101.1	273.8	62.6	0.1	696.5	491.2
	Orchards (OC)	207.7	1.7	11.6	124.0	438.2	338.0	64.6	0.1	1186.0	747.8
	Crops (CR)	309.0	5.2	25.3	79.2	240.1	470.7	175.6	0.3	1305.3	834.6
	Unused (UL)	97.5	1.9	15.5	18.6	54.0	142.1	214.0	0.2	543.7	329.7
	Others (OT)	6.1	0.4	18.3	2.3	15.7	10.4	1.7	0.2	55.0	54.8
	Total	1874.5	35.3	292.6	733.9	1433.4	2085.8	849.8	1.2	7306.6	4630.8
	Reduction	711.1	20.3	123.7	528.5	995.3	1615.2	635.8	0.9	4630.8	

Table 7. Cont.

The 2000–2020 Period		PD	BU	WT	FR	OC	CR	UL	OT	Total	Expansion
2020	Paddy (PD)	1176.3	3.8	52.2	305.5	577.8	820.2	356.2	0.2	3292.2	2115.9
	Built-up (BU)	61.6	23.5	20.2	18.8	75.6	161.2	89.5	0.2	450.7	427.2
	Water (WT)	96.0	2.3	168.0	26.4	56.8	91.0	50.8	0.1	491.3	323.3
	Forest (FR)	36.1	0.4	9.4	123.0	43.9	149.3	40.5	0.1	402.7	279.7
	Orchards (OC)	248.7	1.5	10.5	137.6	444.0	340.4	74.8	0.1	1257.7	813.7
	Crops (CR)	220.8	3.0	19.2	102.2	210.9	452.5	160.9	0.3	1170.0	717.4
	Unused (UL)	34.6	0.8	12.5	19.7	23.8	68.8	75.8	0.1	236.0	160.2
	Others (OT)	0.3	0.1	0.6	0.6	0.7	2.3	1.2	0.0	5.9	5.8
	Total	1874.5	35.3	292.6	733.9	1433.4	2085.8	849.8	1.2	7306.6	4843.2
	Reduction	698.2	11.8	124.6	610.8	989.4	1633.3	773.9	1.1	4843.2	
The 2010–2020 Period		PD	BU	WT	FR	OC	CR	UL	OT	Total	Expansion
2020	Paddy (PD)	1980.0	25.0	79.0	107.1	355.2	529.2	203.1	13.7	3292.2	1312.3
	Built-up (BU)	79.2	87.7	53.5	19.0	47.7	103.0	54.7	5.9	450.7	363.0
	Water (WT)	138.8	8.7	189.0	26.7	29.6	53.1	24.9	20.6	491.3	302.4
	Forest (FR)	62.3	2.2	16.5	220.5	40.3	46.8	12.7	1.5	402.7	182.2
	Orchards (OC)	290.3	11.4	26.1	167.6	472.5	225.6	55.7	8.4	1257.7	785.1
	Crops (CR)	337.8	20.4	34.8	133.2	211.7	303.2	125.1	3.7	1170.0	866.8
	Unused (UL)	52.5	6.1	16.7	21.5	28.7	43.3	66.2	0.9	236.0	169.8
	Others (OT)	0.6	1.0	0.5	1.0	0.3	1.1	1.3	0.1	5.9	5.7
	Total	2941.4	162.5	416.1	696.5	1186.0	1305.3	543.7	55.0	7306.6	3987.4
	Reduction	961.4	74.8	227.2	476.0	713.5	1002.1	1002.1	54.9	4512.0	

For instance, in Table 7, in the 1990–2020 period, out of the total paddy area of 935.0 km² in 1990, 575.3 km² showed no change, whereas 41.7, 51.1, 17.7, 117.7, 113.6, 17.6, and 0.2 km² were lost to the built-up, water, forest, orchard, crops, unused land (UL), and other areas, respectively. As a result, the total reduction area was 359.7 km². In the meanwhile, the total paddy area in 2020 was 3292.2 km². Some areas were gained from the built-up (21.1 km²), water (121.3 km²), forest (429.2 km²), orchards (487.5 km²), crops (701.3 km²), unused land (974.4 km²), other (1.1 km²) areas. Consequently, the total expansion area was 2717.0 km², which accounted for 82.5% of the total paddy area in 2020. For the built-up class, the total area in 1990 was just 18.8 km² (Table 7), however after 30 years, 9.3 km² was stable, whereas 9.5 km² was lost to the paddy (2.1 km²), water (0.9 km²), forest (0.20 km²), orchards (1.0 km²), crops (3.1 km²), unused land (2.0 km²), and other (0.2 km²) areas. Regarding the forest class, after 30 years, an area totaling 906.7 km² was lost, however an area totaling 259.8 km² was gained (Table 7). Spatial patterns of these LULC changes for the Dong Thap Muoi area are shown in Figure 9.

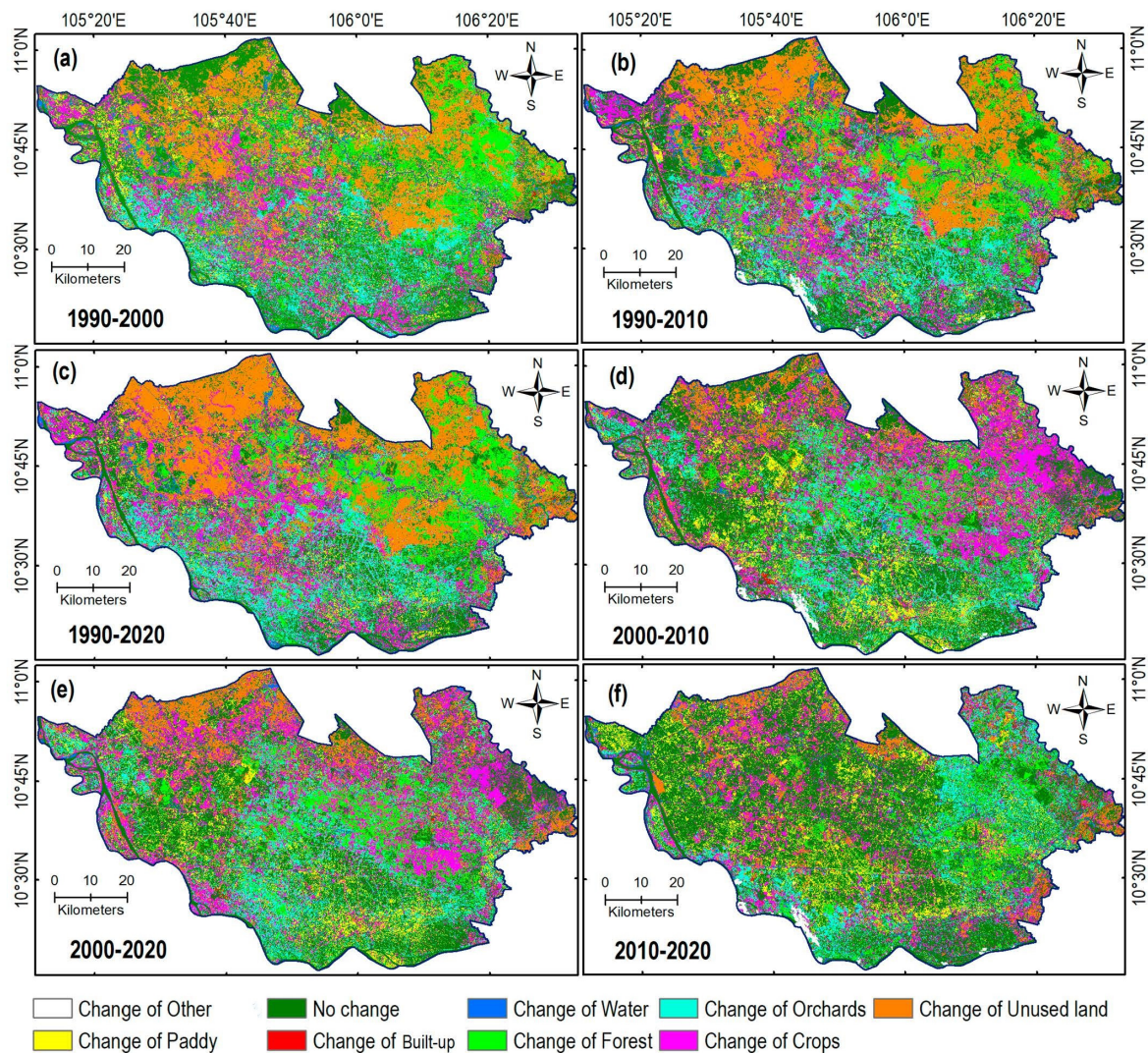


Figure 9. Distribution of LULC changes in the Dong Thap Muoi area for the different periods: (a) 1990–2000; (b) 1990–2010; (c) 1990–2020; (d) 2000–2010; (e) 2000–2020; (f) 2010–2020.

5. Discussion

5.1. Accuracy of the LULC Classification

The Dong Thap Muoi area is influenced by the tropical monsoon climate. Therefore, the collected images were affected by clouds and their shadows, although the Landsat images were collected in the dry season only. In this project, cloud filtering with the C Function of Mask (CFMask) algorithm available at GEE was used for pre-processing, however pixel reconstructions were still required to derive the “fresh” images. The overall accuracy of the LULC maps for 1990, 2000, 2010, and 2020 was higher than 83%, which satisfied the suggested thresholds mentioned by Were et al. [67] for LULC mapping with remotely sensed images. Among the LULC classes, the built-up class had the lowest accuracy, especially in the LULC maps for 2000 and 2010. Herein, built-up pixels were misclassified into the unused land class. However, this is a reasonable result because the built-up class was too fragmented before 2010. Thus, due to the topographical conditions, residence habits, and economic activity relating to wet rice cultivation, the inhabitants are mainly concentrated in towns and clusters along roads and irrigation canals. The misclassification was also due to spectral confusion between the crop and paddy classes (i.e., in 2000). Nevertheless, all LULC classes had user and producer accuracy rates higher than 70%, which are acceptable accuracy levels for the complex nature of LULC changes in

the Dong Thap Muoi area. The kappa index values ranged from 0.835 to 0.889, indicating that the LULC models classified these images better than random images, which ranged from 83.5% to 88.9%.

5.2. LULC Changes

In the 1980s, irrigation canals were constructed to bring fresh water into the area, the process of exploitation was started, and the population began to increase. Due to the topographical conditions, residence habits, and the economic activity related to wet rice cultivation, the inhabitants are mainly concentrated in the towns and clusters along roads and irrigation canals. This analysis indicates that the paddy, unused land, forest, and built-up classes showed the most important LULC changes in the Dong Thap Muoi area during the period 1990–2020. Herein, the unused land and paddy areas had the highest magnitude of changes. During the 30-year period (1990–2020), the unused land decreased by 1877.5 km², and this change accounted for 25.6% of the total studied area. The highest annual rate of change was for the period 1990–2000 at around 126.3 km²/year, whereas the change was more stable for the period 2000–2020.

In 1990, the built-up area totaled for 18.8 km², which accounted for 0.26% of the total Dong Thap Muoi area, however in 2020, the built-up area increased 24 times to 450.7 km² (Table 6). The annual change rate was 14.4 km²/year. The highest change rate per year was for the 2010–2020 period (28.9 km²/year), followed by the 2000–2020 period (20.8 km²/year), the 2000–2010 period (12.7 km²/year), the 1990–2010 period (7.2 km²/year), and the 1990–2000 period (1.7 km²/year). Thus, the population increase was the main cause. The total population in 2001 was 2,463,377 people and the average population density was 337 people/km² [36], however in 2019 the total population was 2,594,211 people. From 2015 to 2019, the total population in the Dong Thap Muoi area increased by 18,730 people [68].

The population growth and increase in exploitation in the Dong Thap Muoi area were in line with the forest cover losses throughout the study period. The forest area totaled 1049.5 km² in 1990 and was consistently reduced to 402.7 km² in 2020 (Table 5).

In 1990, the water body area totaled 403.6 km², which decreased to 292.6 km² in 2000 and then increased to 416.1 km² in 2010 and 491.3 km² in 2020 (Table 7). This is because in the 1990–2000 period, the expansion of agriculture practices was largely spontaneous and uncontrolled. Many wetland areas and natural rivers were used for these agricultural practices, which were considered a cause of flooding in the 2000s in the area, where the network of natural rivers and canals could not adapt to drain water. Then, flood control measures were developed [69,70] for the study area, including clearances of natural flow in rice cultivation areas, which increased the water bodies again.

The orchard land class increased from 1322.0 km² in 1990 to 1433.4 km² in 2000, and then reduced to 1186.0 km² in 2010 and increased again to 1257.7 km² in 2020. Overall, it was reduced by around 4.9%. For the crops classification, this LULC class sharply increased from 1462.4 km² in 1990 to 2085.8 km² in 2010 but was greatly reduced to 1170.0 km² in 2020. In total, it was reduced by around 20% during the 1990–2020 period. Herein, orchard and crop areas were lost mainly to the built-up and paddy areas. Thus, the policies of the local authorities regarding agriculture reconstruction [71,72] were the main reasons for the changes of these two LULC classes, aiming to achieve higher added value and sustainable development in this study area.

5.3. Potential Driving Forces for the LULC Changes

During the years 1975–1980, most of the land in this area was unexploited and acid sulfate soil was dominant and difficult to cultivate [73]. In 1977 constructed started for the freshwater canal, namely the Hong Ngu–Vinh Hung canal, which has a length of 45 km and was completed in 1984. Exploitation then started to occur in this area, whereby people from other regions selected areas located on both sides of the canal to settle down, build houses, cultivate the land, and develop their new lives.

The LULC transformation and the development of Dong Thap Muoi entered a new phase in the years after 1986, which was strongly related to the socioeconomic renovation of the Vietnamese government, called the “Doi Moi” policy [74] in Vietnam. This was especially influenced by directive No. 515-TTg from the Vietnamese government enacted on 10 July 1997, which related to strengthening the implementation of exploitation activities and socioeconomic development in the Dong Thap Muoi area. As a result, the Dong Thap Muoi area was still mostly unexplored until nearly 1990, at which point unused land was dominant, however by 2020 the area had become almost fully exploited.

Changing from an area with harsh natural conditions and a sparsely distributed population, where most people made a living through self-sufficient production that was dependent on nature, Dong Thap Muoi has become an important rice production area. More importantly, irrigation, dike, and road networks have been expanded significantly [70,75,76], which favor the expansion of paddy cultivation. Additionally, the population has been reallocated better and people’s cultural and social lives have been improved.

6. Concluding Remarks

This project assesses the thirty-year dynamics of land cover/land use changes in the Dong Thap Muoi area in Southern Vietnam for the period 1990–2020. A total of 128 scenes, topographic maps, land use status maps, cadastral maps, and ancillary data were adopted to derive the LULC maps. This is the first study to assess in detail the LULC changes in the Dong Thap Muoi area. From the results, we can draw the following conclusions:

- The paddy, built-up, water body, forest, orchard, crops, and unused land classes are the main LULC classes in the Dong Thap Muoi area;
- During the last 30 years, from 1990 to 2020, the paddy and built-up areas have increased greatly, whereas the forest and unused land areas have been significantly reduced. The paddy areas were transformed mainly from unused land areas;
- The LULC analysis results from this study may help the authorities design exploitation policies for the socioeconomic development of the Dong Thap Muoi area in the future;
- Google Earth Engine is a powerful tool for LULC classification;
- Future extensions of this research should focus on assessing the effects of the LULC changes in flood hazards and natural ecosystems in the Dong Thap Muoi area.

Author Contributions: Conceptualization, Nguyen An Binh, Pham Viet Hoa, Nguyen Ngoc An, Tran Anh Phuong, and Dieu Tien Bui; methodology, Pham Viet Hoa, Nguyen An Binh, Dieu Tien Bui; software, Huynh Song Nhut, and Giang Thi Phuong Thao; validation, Nguyen Ngoc An, Tran Anh Phuong, and Nguyen Cao Hanh; formal analysis, Giang Thi Phuong Thao and Tran Anh Phuong; investigation, Huynh Song Nhut, Nguyen Ngoc An, The Trinh Pham, and Le Thi Thu Ha; resources, The Trinh Pham and Le Thi Thu Ha; data curation, The Trinh Pham and Le Thi Thu Ha; writing—original draft preparation, Nguyen An Binh, Pham Viet Hoa, and Dieu Tien Bui; writing—review and editing, Nguyen An Binh and Dieu Tien Bui; visualization, Pham Viet Hong; project administration, Nguyen An Binh and Pham Viet Hong; funding acquisition, Nguyen An Binh and Pham Viet Hoa. All authors have read and agreed to the published version of the manuscript.

Funding: This research was funded by the grant number KHCHN-TNB.ĐT/14-19/C40, which belongs to the Program of Tây Nam Bộ (Vietnam).

Data Availability Statement: The data used in this study are available upon request.

Acknowledgments: This research was partly supported by Program of Tây Nam Bộ (Vietnam) through the project KHCHN-TNB.ĐT/14-19/C40.

Conflicts of Interest: The authors declare no conflict of interest.

References

- Kuenzer, C.; Ottinger, M.; Liu, G.; Sun, B.; Baumhauer, R.; Dech, S. Earth observation-based coastal zone monitoring of the yellow river delta: Dynamics in China's second largest oil producing region over four decades. *Appl. Geogr.* **2014**, *55*, 92–107. [[CrossRef](#)]
- Spruce, J.; Bolten, J.; Mohammed, I.N.; Srinivasan, R.; Lakshmi, V. Mapping land use land cover change in the lower mekong basin from 1997 to 2010. *Front. Environ. Sci.* **2020**, *8*, 21. [[CrossRef](#)]
- Sleeter, B.M.; Liu, J.; Daniel, C.; Rayfield, B.; Sherba, J.; Hawbaker, T.J.; Zhu, Z.; Selmants, P.C.; Loveland, T.R. Effects of contemporary land-use and land-cover change on the carbon balance of terrestrial ecosystems in the United States. *Environ. Res. Lett.* **2018**, *13*, 045006. [[CrossRef](#)]
- Tran, D.X.; Pla, F.; Latorre-Carmona, P.; Myint, S.W.; Caetano, M.; Kieu, H.V. Characterizing the relationship between land use land cover change and land surface temperature. *ISPRS J. Photogramm. Remote Sens.* **2017**, *124*, 119–132. [[CrossRef](#)]
- Findell, K.L.; Berg, A.; Gentine, P.; Krasting, J.P.; Lintner, B.R.; Malyshev, S.; Santanello, J.A.; Shevliakova, E. The impact of anthropogenic land use and land cover change on regional climate extremes. *Nat. Commun.* **2017**, *8*, 989. [[CrossRef](#)] [[PubMed](#)]
- Safaei, M.; Bashari, H.; Mosaddeghi, M.R.; Jafari, R. Assessing the impacts of land use and land cover changes on soil functions using landscape function analysis and soil quality indicators in semi-arid natural ecosystems. *Catena* **2019**, *177*, 260–271. [[CrossRef](#)]
- Garg, V.; Aggarwal, S.; Gupta, P.K.; Nikam, B.R.; Thakur, P.K.; Srivastav, S.; Kumar, A.S. Assessment of land use land cover change impact on hydrological regime of a basin. *Environ. Earth Sci.* **2017**, *76*, 635. [[CrossRef](#)]
- Zope, P.; Eldho, T.; Jothiprakash, V. Impacts of land use–land cover change and urbanization on flooding: A case study of oshiwara river Basin in Mumbai, India. *Catena* **2016**, *145*, 142–154. [[CrossRef](#)]
- Zope, P.; Eldho, T.; Jothiprakash, V. Hydrological impacts of land use–land cover change and detention basins on urban flood hazard: A case study of Poisar River basin, Mumbai, India. *Nat. Hazards* **2017**, *87*, 1267–1283. [[CrossRef](#)]
- Gómez-Aíza, L.; Martínez-Ballesté, A.; Álvarez-Balderas, L.; Lombardero-Goldaracena, A.; García-Meneses, P.M.; Caso-Chávez, M.; Conde-Álvarez, C. Can wildlife management units reduce land use/land cover change and climate change vulnerability? Conditions to encourage this capacity in Mexican municipalities. *Land Use Policy* **2017**, *64*, 317–326. [[CrossRef](#)]
- Hasan, M.H.; Hossain, M.J.; Chowdhury, M.A.; Billah, M. Salinity intrusion in southwest coastal Bangladesh: An insight from land use change. In *Water, Flood Management and Water Security under a Changing Climate*; Springer: Berlin/Heidelberg, Germany, 2020; pp. 125–140.
- Tadese, M.; Kumar, L.; Koech, R.; Kogo, B.K. Mapping of land-use/land-cover changes and its dynamics in Awash River Basin using remote sensing and GIS. *Remote Sens. Appl. Soc. Environ.* **2020**, *19*, 100352.
- Li, J.; Wang, Z.; Lai, C.; Wu, X.; Zeng, Z.; Chen, X.; Lian, Y. Response of net primary production to land use and land cover change in mainland China since the late 1980s. *Sci. Total Environ.* **2018**, *639*, 237–247. [[CrossRef](#)]
- Li, X.; Chen, D.; Duan, Y.; Ji, H.; Zhang, L.; Chai, Q.; Hu, X. Understanding land use/land cover dynamics and impacts of human activities in the Mekong Delta over the last 40 years. *Glob. Ecol. Conserv.* **2020**, *22*, e00991. [[CrossRef](#)]
- Tran, H.; Tran, T.; Kervyn, M. Dynamics of land cover/land use changes in the Mekong Delta, 1973–2011: A remote sensing analysis of the Tran Van Thoi District, Ca Mau Province, Vietnam. *Remote Sens.* **2015**, *7*, 2899–2925. [[CrossRef](#)]
- Paik, S.; Le, D.T.P.; Nhu, L.T.; Mills, B.F. Salt-tolerant rice variety adoption in the Mekong River Delta: Farmer adaptation to sea-level rise. *PLoS ONE* **2020**, *15*, e0229464. [[CrossRef](#)]
- My, N.H.; Demont, M.; Verbeke, W. Inclusiveness of consumer access to food safety: Evidence from certified rice in Vietnam. *Glob. Food Secur.* **2021**, *28*, 100491. [[CrossRef](#)]
- Ngo, K.D.; Lechner, A.M.; Vu, T.T. Land cover mapping of the Mekong Delta to support natural resource management with multi-temporal Sentinel-1A synthetic aperture radar imagery. *Remote Sens. Appl. Soc. Environ.* **2020**, *17*, 100272. [[CrossRef](#)]
- Sakamoto, T.; Van Phung, C.; Kotera, A.; Nguyen, K.D.; Yokozawa, M. Analysis of rapid expansion of inland aquaculture and triple rice-cropping areas in a coastal area of the Vietnamese Mekong Delta using MODIS time-series imagery. *Landsc. Urban Plan.* **2009**, *92*, 34–46. [[CrossRef](#)]
- Hong, H.T.C.; Avtar, R.; Fujii, M. Monitoring changes in land use and distribution of mangroves in the southeastern part of the Mekong River Delta, Vietnam. *Trop. Ecol.* **2019**, *60*, 552–565. [[CrossRef](#)]
- Binh, T.; Vromant, N.; Hung, N.T.; Hens, L.; Boon, E. Land cover changes between 1968 and 2003 in Cai Nuoc, Ca Mau peninsula, Vietnam. *Environ. Dev. Sustain.* **2005**, *7*, 519–536. [[CrossRef](#)]
- Nguyen, H.H.; Dargusch, P.; Moss, P.; Aziz, A.A. Land-use change and socio-ecological drivers of wetland conversion in Ha Tien Plain, Mekong Delta, Vietnam. *Land Use Policy* **2017**, *64*, 101–113. [[CrossRef](#)]
- Veettil, B.K.; Quang, N.X.; Trang, N.T.T. Changes in mangrove vegetation, aquaculture and paddy cultivation in the Mekong Delta: A study from Ben Tre Province, southern Vietnam. *Estuar. Coast. Shelf Sci.* **2019**, *226*, 106273. [[CrossRef](#)]
- Sakamoto, T.; Van Nguyen, N.; Ohno, H.; Ishitsuka, N.; Yokozawa, M. Spatio-temporal distribution of rice phenology and cropping systems in the Mekong Delta with special reference to the seasonal water flow of the Mekong and Bassac rivers. *Remote Sens. Environ.* **2006**, *100*, 1–16. [[CrossRef](#)]
- Le, T.N.; Bregt, A.K.; van Halsema, G.E.; Hellegers, P.J.; Nguyen, L.-D. Interplay between land-use dynamics and changes in hydrological regime in the Vietnamese Mekong Delta. *Land Use Policy* **2018**, *73*, 269–280. [[CrossRef](#)]
- Van, C.T.; Tuyet, N.T.; An, N.V.; Phung, L.V.; Huy, N.P.; Hong, N.M.; Ngoc, N.Q. Assessment of the change of water surface flow in feature points in the Dong Thap Muoi. *J. Meteorol. Hydrol.* **2018**, *8*, 1–7.

27. Hien, M. Links for Sustainable Development of Dong Thap Muoi Sub-Region Online Newspaper of the Government of Vietnam. 2017. Available online: <http://baochinhphu.vn/Hoat-dong-dia-phuong/Lien-ket-phat-trien-ben-vung-Tieu-vung-Dong-Thap-Muoi/304602.vgp> (accessed on 25 September 2020).
28. Nghia, S. Dong Thap Muoi Exploit. Available online: <https://vietnam.vnnet.vn/english/dong-thap-muoi-exploit/200646.html> (accessed on 25 September 2020).
29. MohanRajan, S.N.; Loganathan, A.; Manoharan, P. Survey on land use/land cover (LU/LC) change analysis in remote sensing and GIS environment: Techniques and challenges. *Environ. Sci. Pollut. Res.* **2020**, *27*, 29900–29926. [[CrossRef](#)]
30. Zou, Q.; Li, G.; Yu, W. MapReduce functions to remote sensing distributed data processing—Global vegetation drought monitoring as example. *Softw. Pract. Exp.* **2018**, *48*, 1352–1367. [[CrossRef](#)]
31. Mutanga, O.; Kumar, L. Google Earth Engine Applications. *Remote Sens.* **2019**, *11*, 591. [[CrossRef](#)]
32. Rizvi, S.R.; Killough, B.; Cherry, A.; Gowda, S. Lessons learned and cost analysis of hosting a full stack Open Data Cube (ODC) application on the Amazon Web Services (AWS). In Proceedings of the 2018 IEEE International Geoscience and Remote Sensing Symposium, Valencin, Spain, 22–27 July 2018; pp. 8643–8646.
33. Dong, J.; Metternicht, G.; Hostert, P.; Fensholt, R.; Chowdhury, R.R. Remote sensing and geospatial technologies in support of a normative land system science: Status and prospects. *Curr. Opin. Environ. Sustain.* **2019**, *38*, 44–52. [[CrossRef](#)]
34. Lewis, A.; Oliver, S.; Lymburner, L.; Evans, B.; Wyborn, L.; Mueller, N.; Raevksi, G.; Hooke, J.; Woodcock, R.; Sixsmith, J. The Australian geoscience data cube—Foundations and lessons learned. *Remote Sens. Environ.* **2017**, *202*, 276–292. [[CrossRef](#)]
35. Ghorbanian, A.; Kakooei, M.; Amani, M.; Mahdavi, S.; Mohammadzadeh, A.; Hasanlou, M. Improved land cover map of Iran using Sentinel imagery within Google Earth Engine and a novel automatic workflow for land cover classification using migrated training samples. *ISPRS J. Photogramm. Remote Sens.* **2020**, *167*, 276–288. [[CrossRef](#)]
36. Hoc, D.X. *Study on Flood Drainage and Socio-Economic and Environmental Issues for Sustainable Development in Dong Thap Muoi region*; Thuyloi University, Ho Chi Minh city Campus: Ho Chi Minh City, Vietnam, 2004.
37. Nguyen, N.A. Historic drought and salinity intrusion in the Mekong Delta in 2016: Lessons learned and response solutions. *Vietnam J. Sci. Technol. Eng.* **2017**, *59*, 93–96. [[CrossRef](#)]
38. Yen, B.T.; Son, N.H.; Amjath-Babu, T.; Sebastian, L. Development of a participatory approach for mapping climate risks and adaptive interventions (CS-MAP) in Vietnam’s Mekong River Delta. *Clim. Risk Manag.* **2019**, *24*, 59–70. [[CrossRef](#)]
39. Shrestha, S.; Bach, T.V.; Pandey, V.P. Climate change impacts on groundwater resources in Mekong Delta under representative concentration pathways (RCPs) scenarios. *Environ. Sci. Policy* **2016**, *61*, 1–13. [[CrossRef](#)]
40. MONRE. *Technical Regulation on the Structure Model and Content of the National Spatial Data Infrastructure of the Vietnam Scales 1: 10,000 and 1: 25,000*; Ministry of Natural Resources and Environment Hanoi: Hanoi, Vietnam, 2020.
41. Tien Bui, D.; Tran, C.T.; Pradhan, B.; Revhau, I.; Seidu, R. iGeoTrans—A novel iOS application for GPS positioning in geosciences. *Geocarto Int.* **2015**, *30*, 202–217. [[CrossRef](#)]
42. Jensen, J. *Introductory Digital Image Processing: A Remote Sensing Perspective*, 4th ed.; Pearson: Glenview, IL, USA, 2015.
43. Claverie, M.; Ju, J.; Masek, J.G.; Dungan, J.L.; Vermote, E.F.; Roger, J.-C.; Skakun, S.V.; Justice, C. The harmonized landsat and sentinel-2 surface reflectance data set. *Remote Sens. Environ.* **2018**, *219*, 145–161. [[CrossRef](#)]
44. Li, H.; Wan, W.; Fang, Y.; Zhu, S.; Chen, X.; Liu, B.; Hong, Y. A google earth engine-enabled software for efficiently generating high-quality user-ready landsat mosaic images. *Environ. Model. Softw.* **2019**, *112*, 16–22. [[CrossRef](#)]
45. Vo, Q.T.; Oppelt, N.; Leinenkugel, P.; Kuenzer, C. Remote sensing in mapping mangrove ecosystems—An object-based approach. *Remote Sens.* **2013**, *5*, 183–201. [[CrossRef](#)]
46. Thi, H.P.; Quoc, D.N.; Hoai, T.T.T.; Le Thi, N. Determination of the relationship between Vietnam national coordinate reference system (VN-2000) and ITRS, WGS84 and PZ-90. In Proceedings of the E3S Web of Conferences, Bali, Indonesia, 21–23 November 2018; p. 03014.
47. Liu, C.; Frazier, P.; Kumar, L. Comparative assessment of the measures of thematic classification accuracy. *Remote Sens. Environ.* **2007**, *107*, 606–616. [[CrossRef](#)]
48. Hoa, N.T.P. *Circular of the Regulation on Economic and Technical Levels of the Landuse Statistics and Landuse Status Mapping*; Ministry of Natural Resources and Environment: Hanoi, Vietnam, 2019.
49. FAO. *Land Cover Classification System: Classification Concepts and User Manual. Software Version 2 (Environment and Natural Resources Management Series)*; Food and Agriculture Organization of the United Nations: Rome, Italy, 2008.
50. Homer, C.H.; Fry, J.A.; Barnes, C.A. The national land cover database. *USA Geol. Surv. Fact Sheet* **2012**, *3020*, 1–4.
51. Fortier, J.; Rogan, J.; Woodcock, C.E.; Runfola, D.M. Utilizing temporally invariant calibration sites to classify multiple dates and types of satellite imagery. *Photogramm. Eng. Remote Sens.* **2011**, *77*, 181–189. [[CrossRef](#)]
52. Zhou, W.; Cao, F. Effects of changing spatial extent on the relationship between urban forest patterns and land surface temperature. *Ecol. Indic.* **2020**, *109*, 105778. [[CrossRef](#)]
53. Rodriguez-Galiano, V.F.; Ghimire, B.; Rogan, J.; Chica-Olmo, M.; Rigol-Sanchez, J.P. An assessment of the effectiveness of a random forest classifier for land-cover classification. *ISPRS J. Photogramm. Remote Sens.* **2012**, *67*, 93–104. [[CrossRef](#)]
54. Phalke, A.R.; Özdoğan, M.; Thenkabail, P.S.; Erickson, T.; Gorelick, N.; Yadav, K.; Congalton, R.G. Mapping croplands of Europe, middle east, russia, and central asia using landsat, random forest, and google earth engine. *ISPRS J. Photogramm. Remote Sens.* **2020**, *167*, 104–122. [[CrossRef](#)]

55. Zeferino, L.B.; de Souza, L.F.T.; do Amaral, C.H.; Fernandes Filho, E.I.; de Oliveira, T.S. Does environmental data increase the accuracy of land use and land cover classification? *Int. J. Appl. Earth Obs. Geoinf.* **2020**, *91*, 102128. [[CrossRef](#)]
56. Breiman, L. Random forests. *Mach. Learn.* **2001**, *45*, 5–32. [[CrossRef](#)]
57. Sheykhmousa, M.; Mahdianpari, M.; Ghanbari, H.; Mohammadimanesh, F.; Ghamisi, P.; Homayouni, S. Support vector machine vs. random forest for remote sensing image classification: A meta-analysis and systematic review. *IEEE J. Sel. Top. Appl. Earth Obs. Remote Sens.* **2020**. [[CrossRef](#)]
58. Belgiu, M.; Drăguț, L. Random forest in remote sensing: A review of applications and future directions. *ISPRS J. Photogramm. Remote Sens.* **2016**, *114*, 24–31. [[CrossRef](#)]
59. Batar, A.K.; Watanabe, T.; Kumar, A. Assessment of land-use/land-cover change and forest fragmentation in the Garhwal Himalayan Region of India. *Environments* **2017**, *4*, 34. [[CrossRef](#)]
60. Rodriguez-Galiano, V.; Chica-Olmo, M.; Abarca-Hernandez, F.; Atkinson, P.M.; Jeganathan, C. Random Forest classification of Mediterranean land cover using multi-seasonal imagery and multi-seasonal texture. *Remote Sens. Environ.* **2012**, *121*, 93–107. [[CrossRef](#)]
61. Rodriguez-Galiano, V.F.; Chica-Rivas, M. Evaluation of different machine learning methods for land cover mapping of a Mediterranean area using multi-seasonal Landsat images and digital terrain models. *Int. J. Digit. Earth* **2014**, *7*, 492–509. [[CrossRef](#)]
62. Chan, J.C.-W.; Paelinckx, D. Evaluation of Random Forest and Adaboost tree-based ensemble classification and spectral band selection for ecotope mapping using airborne hyperspectral imagery. *Remote Sens. Environ.* **2008**, *112*, 2999–3011. [[CrossRef](#)]
63. Shirvani, Z. A holistic analysis for landslide susceptibility mapping applying geographic object-based random forest: A comparison between protected and non-protected forests. *Remote Sens.* **2020**, *12*, 434. [[CrossRef](#)]
64. Isaac, E.; Easwarakumar, K.; Isaac, J. Urban landcover classification from multispectral image data using optimized AdaBoosted random forests. *Remote Sens. Lett.* **2017**, *8*, 350–359. [[CrossRef](#)]
65. Colkesen, I.; Kavzoglu, T. Ensemble-based canonical correlation forest (CCF) for land use and land cover classification using sentinel-2 and Landsat OLI imagery. *Remote Sens. Lett.* **2017**, *8*, 1082–1091. [[CrossRef](#)]
66. Foody, G.M. Explaining the unsuitability of the kappa coefficient in the assessment and comparison of the accuracy of thematic maps obtained by image classification. *Remote Sens. Environ.* **2020**, *239*, 111630. [[CrossRef](#)]
67. Were, K.O.; Dick, Ø.B.; Singh, B.R. Remotely sensing the spatial and temporal land cover changes in Eastern Mau forest reserve and Lake Nakuru drainage basin, Kenya. *Appl. Geogr.* **2013**, *41*, 75–86. [[CrossRef](#)]
68. GSO. *Statistical Yearbook of Vietnam*; General Statistics Office of Vietnam: Hanoi, Vietnam, 2019.
69. Le, T.V.; Haruyama, S.; Nhan, N.H.; Cong, T.T.; Long, B.D. The historical flood in 2000 in Mekong River Delta, Vietnam: A quantitative analysis and simulation. *Geogr. Rev. Jpn.* **2007**, *80*, 663–680.
70. Hoa, L.T.V.; Shigeko, H.; Nhan, N.H.; Cong, T.T. Infrastructure effects on floods in the Mekong River Delta in Vietnam. *Hydrol. Process. Int. J.* **2008**, *22*, 1359–1372. [[CrossRef](#)]
71. Hai, T.N.; Phuong, N.T.; Hien, T.T.T.; Bui, T.; Son, V.N.; Wilder, M.N. Research, development and economics of seed production of giant freshwater prawn (*Macrobrachium rosenbergii*): A review. In Proceedings of the Final Workshop of the JIRCAS Mekong Delta Project, Cantho, Vietnam, 23–25 November 2003; pp. 298–306.
72. Ministry of Agriculture and Rural Development. *Regional Environmental Assessment Report on Mekong Delta Intergrated Climate Resilience and Sustainable Livelihoods Project*; Ministry of Agriculture and Rural Development: Hanoi, Vietnam, 2016.
73. Hung, T.V.; Le, P.T.; Tran, V.D.; Hung, N.N. Morphological and physicochemical properties of acid sulfate soils in Dong Thap Muoi. *Can Tho Univ. J. Sci.* **2017**, *2017*, 1–10.
74. Boothroyd, P.; Nam, P.X. *Socioeconomic Renovation in Vietnam: The Origin, Evolution, and Impact of Doi Moi*; IDRC: Ottawa, ON, Canada, 2000.
75. Binh, T.V.; Le Huy Ba, T.T.T.; Huong, L.N. Ecological economic assessment of the production models in different forms of dikes in Dong Thap Muoi area, Vietnam. *Southeast Asian J. Sci.* **2015**, *4*, 38–50.
76. Tran, T.; James, H. Transformation of household livelihoods in adapting to the impacts of flood control schemes in the Vietnamese Mekong Delta. *Water Resour. Rural Dev.* **2017**, *9*, 67–80. [[CrossRef](#)]